Neuro-Oncology

21(8), 981–992, 2019 | doi:10.1093/neuonc/noz028 | Advance Access date 5 February 2019

Low mutation burden and frequent loss of *CDKN2A/B* and *SMARCA2*, but not PRC2, define premalignant neurofibromatosis type 1–associated atypical neurofibromas

Alexander Pemov, Nancy F. Hansen, Sivasish Sindiri, Rajesh Patidar, Christine S. Higham, Eva Dombi, Markku M. Miettinen, Patricia Fetsch, Hilde Brems, Settara C. Chandrasekharappa, Kristine Jones, Bin Zhu, Jun S. Wei, National Intramural Sequencing Center (NISC) Comparative Sequencing Program, National Cancer Institute (NCI) Division of Cancer Epidemiology and Genetics (DCEG) Cancer Genomics Research Laboratory, James C. Mullikin, Margaret R. Wallace, Javed Khan, Eric Legius, Brigitte C. Widemann, and Douglas R. Stewart

Clinical Genetics Branch, DCEG, NCI, National Institutes of Health (NIH), Rockville, Maryland, USA (A.P., D.R.S.); Cancer Genetics and Comparative Genomics Branch, National Human Genome Research Institute, NIH, Rockville, Maryland, USA (N.F.H., S.C., J.C.M.); Genetics Branch, Center for Cancer Research, NCI, NIH, Bethesda, Maryland, USA (S.S., R.P., J.S.W., J.K.); Molecular Characterization & Clinical Assay Development Laboratory, Frederick National Laboratory for Cancer Research, Leidos Biomedical Research, Inc, Frederick, Maryland, USA (R.P.); Children's National Medical Center, Washington, DC, USA (C.S.H.); Pediatric Oncology Branch, Center for Cancer Research, NCI, NIH, Bethesda, Maryland, USA (C.S.H., E.D., B.C.W.); Laboratory of Pathology, NCI, NIH, Bethesda, Maryland, USA (M.M.M., P.F.); Department of Human Genetics, Catholic University Leuven, Leuven, Belgium (H.B., E.L.); Cancer Genomics Research Laboratory, DCEG, NIH, Rockville, Maryland, USA (K.J., B.Z., N.D.C.G.R.L.); NISC, National Human Genome Research Institute, NIH, Rockville, Maryland, USA (N.C.S.P., J.C.M.); Department of Molecular Genetics and Microbiology, UF Genetics Institute, UF Health Cancer Center, University of Florida, Gainesville, Florida, USA (M.R.W.)

Corresponding Author: Douglas R. Stewart, 9609 Medical Center Drive Rm 6E450, Bethesda, MD, 20892 (drstewart@mail.nih.gov).

Abstract

Background. Neurofibromatosis type 1 (NF1) is a tumor-predisposition disorder caused by germline mutations in *NF1*. NF1 patients have an 8–16% lifetime risk of developing a malignant peripheral nerve sheath tumor (MPNST), a highly aggressive soft-tissue sarcoma, often arising from preexisting benign plexiform neurofibromas (PNs) and atypical neurofibromas (ANFs). ANFs are distinct from both PN and MPNST, representing an intermediate step in malignant transformation.

Methods. In the first comprehensive genomic analysis of ANF originating from multiple patients, we performed tumor/normal whole-exome sequencing (WES) of 16 ANFs. In addition, we conducted WES of 3 MPNSTs, copy-number meta-analysis of 26 ANFs and 28 MPNSTs, and whole transcriptome sequencing analysis of 5 ANFs and 5 MPNSTs.

Results. We identified a low number of mutations (median 1, range 0–5) in the exomes of ANFs (only *NF1* somatic mutations were recurrent), and frequent deletions of *CDKN2A/B* (69%) and *SMARCA2* (42%). We determined that polycomb repressor complex 2 (PRC2) genes *EED* and *SUZ12* were frequently mutated, deleted, or downregulated in MPNSTs but not in ANFs. Our pilot gene expression study revealed upregulated *NRAS*, *MDM2*, *CCND1/2/3*, and *CDK4/6* in ANFs and MPNSTs, and overexpression of *EZH2* in MPNSTs only.

Conclusions. The PN-ANF transition is primarily driven by the deletion of *CDKN2A/B*. Further progression from ANF to MPNST likely involves broad chromosomal rearrangements and frequent inactivation of the PRC2 genes, loss of the DNA repair genes, and copy-number increase of signal transduction and cell-cycle and pluripotency self-renewal genes.

Key Points

1. ANFs are relatively chromosomally stable tumors with low somatic mutation burden.
2. Frequent inactivation of *NF1, CDKN2A/B*, and *SMARCA2* genetically defines ANF.
3. Unlike MPNST, we detect no recurrent PRC2 gene inactivation in ANF.

Importance of the Study

NF1-associated ANFs are rare premalignant lesions with a high risk of transformation to MPNST, a soft-tissue sarcoma with poor prognosis. Early detection and treatment of ANF may prevent MPNST, for which surgery remains the only therapeutic option. At present, the genetics of ANF development and transformation to MPNST are not fully understood. Here we present the first multisample/multipatient comprehensive genomic study of ANF. We show that somatic mutation burden and genomic instability in ANF is relatively low, with only *NF1*, *CDKN2A/B*, and, to a lesser extent, *SMARCA2* mutated in the tumors. *SUZ12, EED*, and *TP53*, which are frequently inactivated in MPNST, are intact in ANF. We conclude that in ANF, loss of *CDKN2A/B* is the main genetic event that in addition to *NF1* inactivation leads to premalignancy. The transition to MPNST coincides with a dramatic rise in genomic instability, inactivation of PRC2, and copy-number gains of cell-cycle and pluripotency genes.

Neurofibromatosis type 1 (NF1) is a common (~1/2000–1/3500 worldwide[1]) autosomal dominant, archetypal tumor-predisposition disorder secondary to mutations in the tumor suppressor *NF1*. Phenotypically, NF1 is associated with neurocutaneous abnormalities, including a variety of benign and malignant tumors.[2] Life expectancy is reduced by 8–15 years in both men and women, primarily due to malignancy and cardiovascular disease.[3,4] A significant proportion of the excess mortality in NF1 is attributable to malignant peripheral nerve sheath tumors (MPNSTs), an aggressive soft-tissue sarcoma with limited therapeutic options.[4] The relative risk of MPNST in NF1 is enormously increased (~2000-fold), with a lifetime risk of 8–16%.[4,5]

MPNSTs typically arise from a preexisting plexiform neurofibroma (PN), a histologically benign congenital neurofibroma affecting up to 50% of people with NF1[6] and readily identified on whole-body MRI.[7] More widespread use of whole-body MRI has prompted the identification of "distinct nodular lesions" (DNLs), frequently within PNs. These lesions are >3 cm in longest diameter, well demarcated, and distinct from surrounding tissue and lack the "central dot" sign of PN. Distinct nodular lesions appear after early childhood and typically grow faster than the surrounding or adjacent PN and may be precursors of an MPNST.[8] Some DNLs are biopsy-proven atypical neurofibromas (ANFs).[9] ANFs are pathologically defined lesions that have increased variable cellularity, cytological atypia, and more pronounced fascicular growth patterns, but lack the widespread atypia and fascicular growth mitotic activity and necrosis seen in MPNST. In one study, 15/16 ANFs harbored a deletion of chromosome 9p21.3, a region that includes cell-cycle regulators cyclin-dependent kinase inhibitor 2A and 2B (*CDKN2A/B*),[10] both frequently deleted somatically in MPNSTs.[11–14]

ANF is hypothesized to be a premalignant lesion, with *CDKN2A/B* deletion the first step in the progression to MPNST. Whole-exome sequencing (WES) and copy-number analysis of PNs showed remarkably low somatic mutation rates, stable chromosomal architecture, and intact *CDKN2A/B* and revealed the primacy of *NF1* inactivation in its pathogenesis.[15] WES of NF1-associated MPNST shows that biallelic loss of *NF1* and mutation in polycomb repressive complex 2 (PRC2) genes are essential to its pathogenesis.[16–18] It remains unclear what other genes and pathways play a role in PN transformation into a premalignant state. Resection of ANF may prevent MPNST[9]; therefore, identification of genetic biomarkers for ANF is important for the disease management. A better understanding of the PN-to-MPNST transformation is a key recommendation from a recent international consensus meeting on research priorities in MPNST.[19,20] To investigate this, we characterized ANFs and a small set of MPNSTs using WES, whole transcriptome sequencing, and copy-number determination.

Materials and Methods

Sample Collection and Clinical Information

Clinical information and tumor samples with matching normal DNA were collected at the NCI in Bethesda, Maryland, the University of Leuven in Belgium, and the University of Florida in Gainesville. The diagnosis of all ANF cases was confirmed by one pathologist at NCI and one pathologist at the University of Leuven. All protocols were approved by the appropriate investigational review board, and subjects and/or their parents or guardians provided written, informed consent. Detailed description of

the materials and methods used in this study can be found in the Supplementary material.

Whole-Exome Sequencing of Matching Pairs of Tumor and Normal DNA

Capture of the exome and library preparation was done using the SeqCap EZ Exome plus UTR Library kit (Roche, #06740308001). Sequencing was done according to the manufacturer's instructions. Among sequenced exomes, the average breadth of coverage was 89% of targeted bases (range 88–91%), and the average depth of coverage was 59x (range 44–82x) for both tumor and normal samples.

Whole-Exome Sequencing Analysis

Sequencing reads were aligned to the National Center for Biotechnology Information's Build GRCh37 (hg19) using Novoalign v2.08.02 (for ANF1 through ANF7) and v3.02.07 (for ANF8 through ANF15). Point mutations and small indels were called for all tumor/normal pairs with Mutect (v1.1.4),[21] SomaticSniper (v1.0.5),[22] and Shimmer (v0.1.1).[23] Mutect and Shimmer used default parameters; filtering of SomaticSniper variants was as per program authors. MPNST samples were analyzed in the same manner, except that an additional somatic caller, Strelka v1.0.14,[24] was added to the pipeline. Coding variants identified as somatic mutations by at least one caller were further filtered by comparing them with 1000 Genomes (internationalgenome.org), ExAC (exac.broadinstitute.org), ESP6500 (evs.gs.washington.edu), and ClinSeq (https://www.ncbi.nlm.nih.gov/projects/gap/cgi-bin/study.cgi?study_id=phs000971.v1.p1, Accessed March 1, 2019) databases; variants with minor allele frequency >1% were removed from further consideration. Variants in known false-positive genes[25] were excluded from further consideration.

Somatic Mutation Verification and Deep *NF1* Mutation Detection by AmpliSeq/Ion Torrent

Multiplex PCR primers for somatic mutation verification were designed using the Ion AmpliSeq Designer tool (v3.0.1, Life Technologies). Multiplex PCR amplification, library preparation, and sequencing on the Ion Proton sequencer (Life Technologies) were performed as per the manufacturer's instructions.

Copy-Number Variation and Loss of Heterozygosity

Single nucleotide polymorphism (SNP) genotyping was performed using HumanOmniExomeExpress BeadChip kits (Illumina, #20004207) as per the manufacturer's instructions. Analysis by allele-specific copy-number analysis of tumors (ASCAT, v2.1) was performed as previously described.[26] For samples ANF1–ANF7, SNP-array data were not available. To analyze somatic copy-number alterations in the *NF1* and *CDKN2A/B* loci in these samples, we used ExomeCNV (v1.4)[27] with the WES data. A copy-number variation (CNV) meta-analysis using previously published data[10] was performed. Paired CNV and loss-of-heterozygosity analysis of tumor and matching normal DNA was performed by using Nexus v6.1 software (BioDiscovery) as described previously.[28] Analysis by Genomic Identification of Significant Targets in Cancer (GISTIC) (https://software.broadinstitute.org/software/cprg/?q=node/31, Accessed March 1, 2019) was performed using the GISTIC module in Nexus v6.1 software.

Whole Transcriptome RNA Sequencing and Analysis of the Data

Total RNA isolation, library construction, and sequencing on the Illumina platform was done as previously described.[15] Expression data were analyzed with Gene Set Enrichment Analysis (GSEA) v2 (Broad Institute; software.broadinstitute.org/gsea) according to the developer's recommendations.

Immunohistochemical Staining of Tumors

All immunohistochemical (IHC) stains were done on formalin-fixed paraffin embedded 5-micron tissue sections mounted on charged microscopic slides.

Results

Clinical Characteristics of Patients and Tumors

Clinical information for the tumors and NF1 patients is summarized in Table 1 and a recent publication.[9] The pathologic classification of ANF was done prior to the development of the new proposed term "atypical neurofibromatous neoplasms of uncertain biologic potential."[20] Hematoxylin and eosin preps of select atypical neurofibromas are shown in comparison to PN and MPNST in Supplementary Figure 1. While normal nuclei and typical plexiform architecture could be observed in PN, multiple instances of nuclear atypia, increased cellularity, and loss of neurofibroma organization are prominent in the ANFs. On the other hand, in high-grade MPNST, multiple mitotic figures and a high degree of cellularity are well distinguished.

NF1, *CDKN2A/B*, and PRC2 Mutational and Copy-Number Status in ANFs and MPNSTs

Information for the analyses performed on the tumor samples is available in Supplementary Table 1. We first sought mutations or deletions in *NF1* and *CDKN2A/B* (Table 2). We identified 14/14 (100%) and 13/16 (81%) *NF1* germline and somatic mutations, respectively, in the 16 ANFs. We identified no point mutations or small indels in *CDKN2A* or *CDKN2B*; however, SNP-array and ExomeCNV analyses revealed hetero- or homozygous loss of the *CDKN2A/2B* locus (9p21.3) in 12/16 (75%) tumors. We sought, but did not find, damaging somatic variation in PRC2 genes (embryonic ectoderm development [*EED*], suppressor of zeste 12 homolog [*SUZ12*], *EZH1/2, RBBP4/7, AEBP2, JARID2*) or in *TP53*.

Table 1. Clinical information for patients and tumors

Tumor Sample ID	Tumor ID in Higham et al, 2018	Tumor Type	Age at Diagnosis, y	Sex	Inheritance	Family History of MPNST	Personal History of MPNST	Location	Reason for Biopsy/ Resection	Additional Concerning Lesions	Isolated or within Plexiform
A15_ANF1	BEL-13-1	ANF	26.9	M	Unknown	NA	No	Neck	G	Yes	Isolated
ANF2	BEL-17	ANF	34.4	F	de novo	No	Yes	Neck	P, G	No	Isolated
A13_ANF3	BEL-11	ANF	58.8	F	Unknown	NA	No	Neck	P, G, E	No	Isolated
A4_ANF4	BEL-4	ANF	28.3	M	Familial-maternal	NA	Yes	Abdomen/ Pelvis	E	No	Unknown
A7_ANF5	N/A	ANF	18.8	F	de novo	No	No	Chest	G, E	No	Within PN
ANF6	BEL-16	ANF	32.7	F	Unknown	NA	No	Lower extremity	P	No	Within PN
A11_ANF7	N/A	ANF	26.7	F	Familial-maternal	No	Yes	Neck	P	Yes	Unknown
ANF8	BEL-14	ANF	28.3	F	Familial-maternal	NA	No	Chest	P, G	No	Unknown
ANF9	N/A	ANF	26.4	M	Familial-maternal	NA	No	Lower extremity	P	No	Unknown
ANF10	BEL-18	ANF	31.8	F	Unknown	NA	No	Chest	G, E	No	Isolated
ANF11-1[a]	NCI-14-3	ANF	28.3	M	Familial-paternal	No	No	Abdomen/ pelvis	G, E	Yes	Within PN
ANF11-2[a]	NCI-14-3	ANF	28.3	M	Familial-paternal	No	No	Abdomen/ pelvis	G, E	Yes	Within PN
ANF11-6	NCI-14-4	ANF	30.4	M	Familial-paternal	No	No	Lower extremity	E	Yes	Isolated
ANF11-7	NCI-14-1	ANF	25.4	M	Familial-paternal	No	No	Abdomen/ pelvis	G, E	Yes	Within PN
ANF13-1	NCI-15	ANF	26	F	Familial-paternal	Yes	Yes	Lower extremity	G, E	Yes	Isolated
ANF14-1[b]	N/A	NF/ ANF[&]	9.4	M	de novo	No	No	Abdomen/ pelvis	G, E	No	Within PN
ANF14-2[b]	NCI-2	ANF	9.4	M	de novo	No	No	Abdomen/ pelvis	G, E	No	Within PN
ANF15	NCI-3	ANF	13.7	M	Familial-maternal	Yes	No	Lower extremity	G, E	Yes	Isolated
MPNST1	N/A	MPNST	17.1	M	Familial-maternal	No	Yes[d]	Abdomen/ pelvis	P, G, E	No	Within PN
MPNST2	N/A	MPNST	47	M	de novo	No	Yes	Upper extremity	P, G	No	Within PN
MPNST3-1[c]	N/A	MPNST	23.6	M	de novo	No	Yes[d]	Abdomen/ pelvis	P, G, E	Yes	Within PN
MPNST3-2[c]	N/A	MPNST	23.6	M	de novo	No	Yes[d]	Abdomen/ pelvis	P, G, E	Yes	Within PN
MPNST4	N/A	MPNST	28	M	de novo	No	Yes	Lower extremity	P, G	No	Within PN
MPNST5	N/A	MPNST	39	M	de novo	No	Yes	Brain metastasis[e]	Neurological symptoms	No	Brain metastasis

Abbreviations: NA = not available, N/A = not applicable; P = pain associated with tumor; G = tumor growth; E = elevated standard uptake value (SUV) on fluorodeoxyglucose-positron emission tomography (FDG-PET); F = female; M = male. Superscripts: [a]fragments of a larger tumor; [b]2 distinct nodular lesions within the same PN; [c]fragments of a larger tumor; [d]lesions included in this study; [e]primary MPNST in a leg; [&]tumor ANF14-1 was initially classified as neurofibroma (NF) by a pathologist; however, based on clinical (fast growth and elevated SUV on FDG-PET scan) and genetic (deletion of the *CDKN2A/B* locus) evaluations in this study, this tumor was reclassified as ANF. IDs for ANF investigated in Higham et al, 2018 (*Neuro-Oncology, Vol. 20, pp. 818–825*) are shown in the second column.

In MPNSTs, we found pathogenic *NF1* germline and somatic mutations/deletions in 4/4 (100%) samples. There was heterozygous or homozygous loss of the *CDKN2A/B* locus in 4/4 (100%) MPNSTs. Like ANFs, we did not identify point mutations or small indels at this locus. We identified a potentially deleterious homozygous missense mutation in *EED* (but intact *SUZ12*) in MPNST4 and a frame-shifting homozygous indel in *SUZ12* in

Table 2. Mutation and CNV in *NF1, CDKN2A/B*, and PRC2 genes in ANF and MPNST

Sample ID	*NF1*, Germline	*NF1*, Somatic	*CDKN2A/2B*	PRC2 Genes
A15_ANF1	Frameshift, p.M991Ifs*2	Gains with multiple breakpoints[b]	Not detected	Not detected
ANF2[a]	Missense, p.A706F	Not detected	Not detected	Not detected
A13_ANF3	Splicing, c.3113+1G>A	Frameshift, p.E2624Rfs*33	Het loss	Not detected
A4_ANF4	Type I microdeletion	Nonsense, p.Q1801X	Not detected	Not detected
A7_ANF5	Frameshift, p.F199Lfs*5	Large deletion	Homozygous loss	Not detected
ANF6[a]	Exons 2-28 deletion	Not detected	Not detected	Not detected
ANF7	Splicing, c.3113+1G>A	Frameshift, p.D2614Nfs*7	Homozygous loss	Not detected
ANF8	Missense, p.L2317P	Large deletion[b]	Het loss	Not detected
ANF9	Missense, p.Y575C NM_001128147	Missense, p.C845Y	Partial gain, with a breakpoint in *CDKN2A*	Not detected
ANF10	Splicing, c.1261-1G>A	Frameshift, p.V224fs*0	Homozygous loss	Not detected
ANF11-1	Frameshift, p.N1582Kfs*19	Copy-neutral LOH	Het loss	Not detected
ANF11-2	Same as in ANF11-1	Copy-neutral LOH	Het loss	Not detected
ANF13	Nonsense, p.R416X	Not detected	Het loss	Not detected
ANF14-1	Splicing, c.288+2T>G	Frameshift, p.I1381Mfs*3	Het loss	Not detected
ANF14-2	Same as in ANF14-1	Same as in ANF14-1	Het loss	Not detected
ANF15	Frameshift, p.T2264Tfs*4	Frameshift, p.K2643Rfs*14	Partial gain, with a breakpoint in *CDKN2A*	Not detected
MPNST1	Nonsense, p.R440X	Frameshift, p.L996Sfs*15	Homozygous loss	Not available
MPNST2	Nonsense, p.R1276X	Copy-neutral LOH	Homozygous loss *CDKN2A*, Het loss *CDKN2B*	Not detected, but *SUZ12* expression is sharply decreased
MPNST3-1	Frameshift, p.Q2050Hfs*10	Large deletion	Het loss	*SUZ12*, p.T415Gfs*4, homozygous
MPNST4	Frameshift, p.N1229Mfs*10	Copy-neutral LOH	Homozygous loss	*EED*, p.S241R, homozygous
Detection rate in ANF	**100% (14/14)**	**81% (13/16)**	**75% (12/16)**	**0% (0/16)**
Detection rate in MPNST	**100% (4/4)**	**100% (4/4)**	**100% (4/4)**	**67% (2/3)**

Abbreviations: Het = heterozygous; LOH = loss of heterozygosity. Superscripts: [a]only ExomeCNV (v1.4) analysis of the WES data for the *NF1* and *CDKN2A/B* loci was performed; [b]copy-number changes detected in WES data only.

MPNST3-1. In MPNST2, no PRC2 genes were mutated; however, expression of *SUZ12*, as demonstrated by RNA sequencing (RNAseq) analysis, was sharply reduced in this tumor, implying that in some cases epigenetic inactivation of PRC2 genes could be at play (Supplementary Figure 2A). The RNAseq findings for *SUZ12* expression in the MPNSTs were confirmed by IHC staining with anti-SUZ12 antibodies: We observed robust SUZ12 expression in MPNST4 and sharply reduced levels of the protein in MPNST2 (Supplementary Figure 2B). Interestingly, in MPNST3, in which *SUZ12* carried a homozygous frameshifting indel and in which the *SUZ12* RNA expression was at ~50% of normal (Supplementary Figure 2A), we observed substantial tumor heterogeneity, with distinct areas in the tumor biopsy exhibiting drastically varying levels of SUZ12 expression (Supplementary Figure 2B). It appears that in some MPNST3 cells the mutant protein is still expressed; however, it is likely that its function is affected by this truncating mutation.

We observed a particularly informative case of a 9-year-old NF1 patient with a PN involving the right inguinal area, pelvis, and thigh (Figure 1). MRI evaluation at NCI revealed 2 DNLs in the inguinal and paraspinal areas. Core biopsies of the inguinal and paraspinal lesions were classified as an ANF and neurofibroma, respectively. The inguinal lesion was later resected and the paraspinal tumor was observed. Genetic analysis of the paraspinal (ANF14-1) and inguinal nodular lesions (ANF14-2) confirmed that they originated within the same PN, since they shared the same second hit in *NF1*. However, ANF14-1 and ANF14-2 harbor distinct deletions of chromosome 9p, which includes *CDKN2A/B* (Supplementary Figure 3). These observations suggest that ANF14-1 and

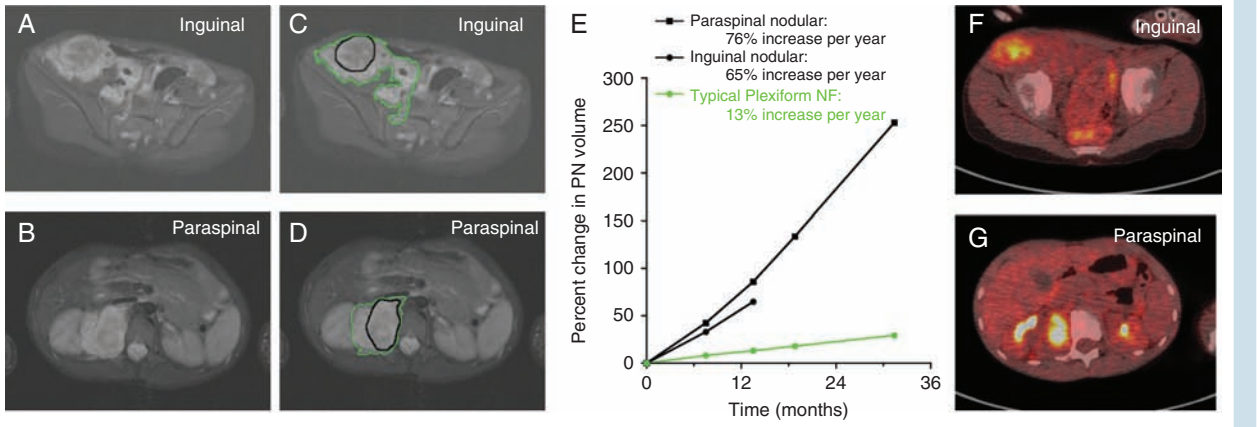

Fig. 1 MRI and fluorodeoxyglucose (FDG) PET evaluation of 2 distinct nodular lesions within a single large PN. (A, B) A 9-year-old boy with NF1 and newly diagnosed PN involving the right retroperitoneum, pelvis, and thigh. MRI evaluation at the NCI revealed 2 distinct nodular lesions, one in the right inguinal area (A; sample ANF14-2), and one in the right paraspinal area (B; sample ANF14-1). (C–E) Volumetric MRI analysis demonstrated faster growth rates for the nodular lesions (black contour) compared with the PN (green contour). (F, G) FDG-PET demonstrated FDG avidity of the nodular lesions with minimal uptake in the surrounding PN (F and G, inguinal and paraspinal lesions, respectively). Core biopsy of the inguinal lesion showed ANF; core biopsy of the paraspinal lesion showed neurofibroma. The inguinal lesion was resected, and pathology confirmed atypical neurofibroma. Follow-up with MRI continues to demonstrate more rapid growth of the remaining paraspinal lesion compared with the PN (C, D).

ANF14-2 arose within the PN and that deletion of *CDKN2A/B* is a predominant driving event in this transformation.

Small-Scale Somatic Mutations in ANF and MPNST Exomes

We identified 13 somatic mutations in 13 genes in 9 ANFs (Supplementary Table 2A). Of the 13 mutated genes, one (*FOXP1*) belonged to the cancer genes in the census of COSMIC (Catalogue of Somatic Mutations in Cancer). One tumor (ANF8) harbored 5 mutations in 5 different genes, 3 of which were predicted to be damaging. All mutations in ANFs were heterozygous, with a median variant allele frequency (VAF) of 0.21 (range 0.18–0.34); *NF1* was the only recurrently mutated gene.

In contrast to ANFs, we observed 70 somatic mutations in 3 MPNSTs, 34 of which were potentially deleterious (Supplementary Table 2B). Unlike ANF mutations, 19/70 mutations in MPNSTs were homozygous (including *EED* and *SUZ12*), and the median VAF was 0.51 (range 0.15–1.00). One gene, *KAT7*, was mutated twice in a single tumor (MPNST2), but both mutations were in *cis*. *NF1* and PRC2 genes (*EED* and *SUZ12* in MPNST4 and MPNST3, respectively) were the only genes found recurrently mutated in the MPNSTs.

Chromosomal Landscape of ANF and MPNST as Revealed by ASCAT Analysis

Next, we used ASCAT to determine allele-specific copy number in 10 ANFs and 4 MPNSTs. Most ANFs were diploid, except for a single tumor (ANF13), which was nearly tetraploid. The median value of the fraction of atypical cells containing CNV in the ANFs was 40.5% (range 22–100%) (Supplementary Figure 4A). Two of the MPNSTs (MPNST1 and MPNST2) were polyploid (4.03 and 4.82, respectively), while MPNST3 and MPNST4 were nearly diploid (1.72 and 1.91). The median proportion of aberrant cells in the MPNSTs was 96% (range 91–99%) (Supplementary Figure 4B).

CNV Meta-Analysis of the Combined ANF Set

Next, we characterized individual CNVs in the combined set of 26 ANFs using Nexus and GISTIC analyses (Figure 2). In 17/26 ANFs (65%), the most frequently affected locus was in 9p21.3, which harbors *CDKN2A/B* (Figure 2B and Supplementary Figure 5A). Most deletions were heterozygous. One deletion in one sample (A2) was called homozygous by the Nexus software, and an additional 6 samples (A7_ANF5, A9, A12, A14, A16, and ANF10) had probe median log2R ratio values considerably lower than the rest of the samples with the deletion (<–0.7), suggesting that the *CDKN2A/B* deletion in these samples was homozygous as well, a finding masked by heterogeneity of the tumors. We found several other regions adjacent to the *CDKN2A/B* locus on 9p that were deleted in more than one-third of the samples, but most of these regions were part of the larger deletion spanning *CDKN2A/B*, implying that the majority of genes within these CNVs might simply be passengers (Figure 2B). We identified one exception: Switching-defective/sucrose nonfermentable (SWI/SNF) related, matrix associated, actin dependent regulator of chromatin, subfamily A2 (*SMARCA2*) was heterozygously deleted in 42% of samples. In ~12% of ANFs (A11_ANF7, A12, ANF11-7), the deletion was clearly independent from *CDKN2A/B* locus loss (Supplementary Figure 2B),

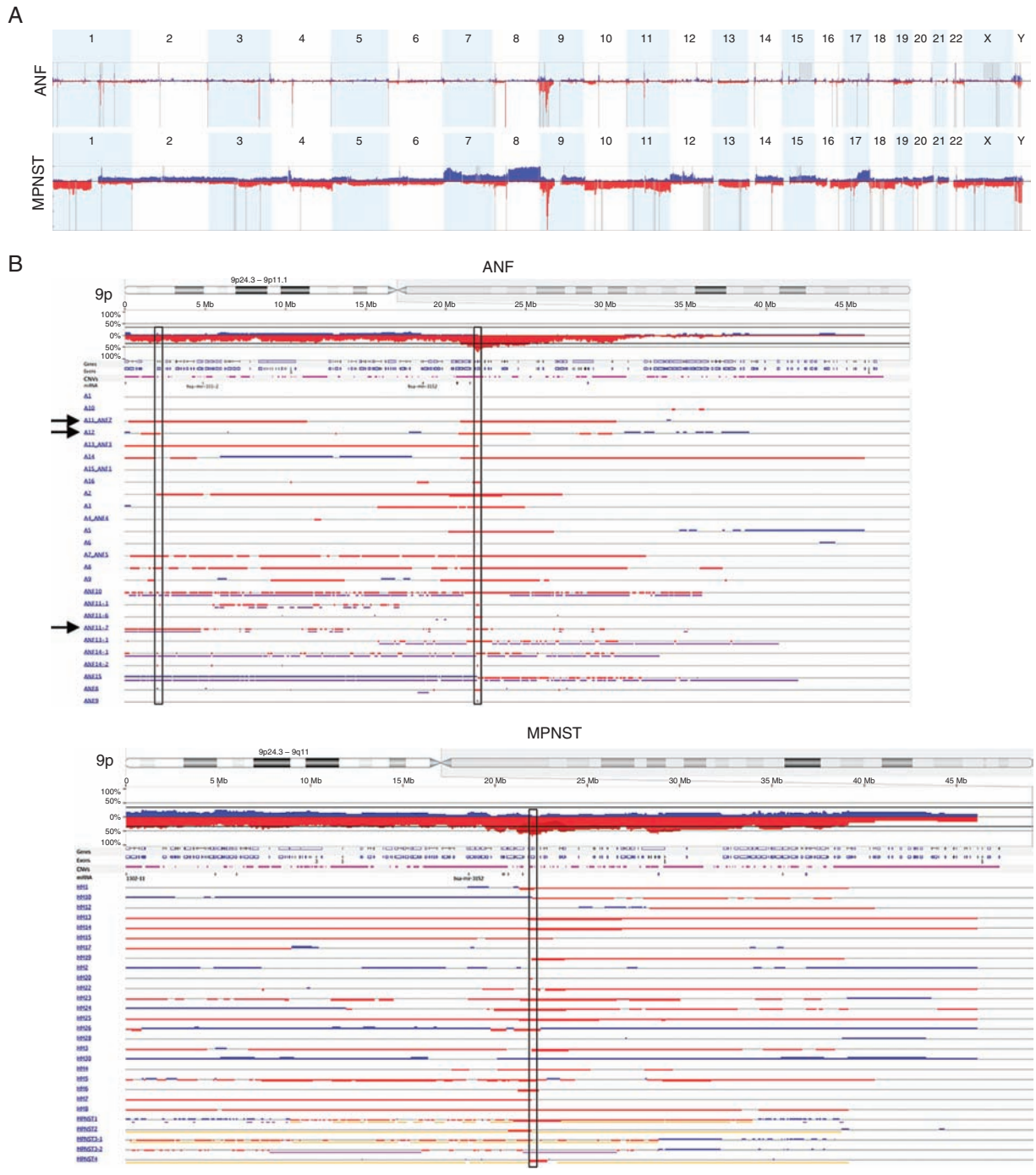

Fig. 2 CNV in ANF and MPNST. (A) GISTIC analysis of 26 ANFs (upper panel) and 28 MPNSTs (lower panel). Gains and losses are shown in blue and red, respectively. Statistically significant CNVs (false discovery rate <0.25) are denoted with gray vertical bars. Chromosome numbers are shown on top of each panel. (B) CNV in chromosome 9p in 26 ANFs (left panel) and 28 MPNSTs (right panel). Gains and losses are shown in blue and red, respectively. Homozygous losses are shown in dark red and thick bars. Vertical rectangles in the center denote minimally overlapped regions in ANF and MPNST that both include the *CDKN2A* and *CDKN2B* genes. Left vertical rectangle in the ANF panel denotes *SMARCA2*. Arrows show samples (A11 ANF7, A12, ANF11-7) in which deletion of *SMARCA2* is clearly independent from *CDKN2A/B*.

suggesting a causative role of SWI/SNF complex disruption in tumor progression.

Among all ANFs, we identified 253 genes that were affected in at least 4/26 samples. Eleven of these 253 genes, including *CDKN2A*, were cancer genes (Supplementary Table 3A–C). One of them, *FANCG*, is a DNA repair protein implicated in maintenance of chromosome architecture (www.uniprot.org), Accessed March 1, 2019 frequent

deletion of this gene could increase genomic instability, a common feature in MPNST. Another gene, *PTPRD*, is a tumor suppressor and a negative regulator of the *STAT3* oncogene.[29] A frequent loss of *PTPRD* or *FANCG* in ANF warrants further investigation. The role of other genes (eg, *JAK2, PDCD1LG2, PSIP1, FCGR2B*) that are predominantly deleted in ANF but are known as oncogenes or fusion genes is more challenging to define. It appears these genes are more likely to be passengers (Supplementary Table 3B).

CNV Meta-Analysis of the Combined MPNST Set

We observed a highly rearranged genomic architecture in the MPNSTs (Figure 2, Supplementary Figure 5B). Like the ANFs, the *CDKN2A/B* locus was one of the most frequently deleted loci (20/28 [71%]) (Figure 2B). Moreover, we observed a homozygous deletion of this locus in 14/28 (50%) samples, which was the most frequently observed homozygous loss in these tumors (Figure 2B).

Across all samples, there were 23 229 genes (including non-coding RNA genes) affected by gains or losses in the regions that overlapped in at least 4/28 samples; 700 were cancer genes (Supplementary Table 3D–F). Out of these 700 genes, we identified 178 oncogenes that were at increased copy-number state, and 144 tumor suppressor genes (TSGs) that were hetero- or homozygously deleted in at least 4/28 samples (Supplementary Table 3E, F). We observed copy-number gains in receptor tyrosine kinase genes that control cellular circuitry, including Ras–mitogen-activated protein kinase (MAPK), phosphatidylinositol-3 kinase–Akt, phospholipase C gamma–protein kinase C, and Janus kinase/signal transducers and activators of transcription pathways (eg, *EGFR, ERBB2/3/4*); signal transduction kinases/phosphatases (eg, *BRAF, AKT2/3*); G1-S phase transition genes (eg, *CDK6, CCND1/3*); negative regulators of TP53 (*PPM1D, MDM2/4*), and telomerase reverse transcriptase, among others. We detected gains and amplifications in *MYC* in 71% of samples and the transcriptional activator of *MYC*, *TRRAP*, was gained in 46% of samples. In addition to *MYC*, we identified increased copy number of *KLF4* and *SOX2*, the genes involved in maintaining "stemness" and pluripotency. *EZH2*, the methyltransferase subunit of PRC2, was found at elevated copy-number state in 50% of MPNSTs.

In addition to multiple gains in oncogenes, we observed a number of losses in TSGs, including DNA repair/recombination genes (eg, *ATM, PALB2*); chromatin modification genes, including PRC2 *EED* and *SUZ12* and subunits of chromatin remodeling complex SWI/SNF (*ARID1A, PBRM1*), and genes controlling pluripotency of stem cells (*ZFHX3, JAK1, BMPR1A, AXIN1, TCF3, TBX3*).

GISTIC Analysis of ANF and MPNST

We identified statistically significant CNVs (false discovery rate <0.25) in 26 ANFs and 28 MPNSTs by GISTIC (Figure 2A, Supplementary Table 3G). Frequent loss of the *CDKN2A/B* locus was confirmed in both types of tumors. In MPNST, we confirmed frequent gain of oncogenes *MDM2* and *PDGFRA* and frequent loss of PRC2 genes *EED* and *SUZ12.*

Significant Increase in Genomic Instability in Transition from ANF to MPNST

We compared the median number of CNVs, median CNV size, median number of bases in all CNVs combined in a tumor and the affected portion of the genome in ANF and MPNST (Table 3). There was a ~7-fold increase in the median number of CNV, a ~4-fold increase of the median size of CNV, and a 33-fold increase of the affected portion of the genome (expressed either as a number of bases or percent of the genome) in MPNST versus ANF. *P*-values for all comparisons were $<10^{-5}$ (Mann–Whitney test), indicating a substantially and significantly increased level of genomic instability in the transition from premalignant to malignant state.

Analysis of Genome-Wide Expression RNAseq Data by GSEA

We analyzed differential expression in ANFs and MPNSTs versus normal tissues using GSEA. Significant gene sets upregulated in ANF related to the immune response, signal transduction, and processes affected in various types of cancer. Downregulated gene sets in ANF were associated with oxidative phosphorylation and cellular respiration. Upregulated gene sets in MPNST were associated with cell cycle, DNA replication/repair, and chromosomal organization, while downregulated gene sets often included genes that were underexpressed in tumors with activated KRAS (Supplementary Table 4). There was a minimal overlap between significant gene sets in ANF and MPNST (data not shown).

Next, we identified up- and downregulated genes in ANF and MPNST that contributed to the enrichment score by performing leading edge analysis. There were 2075 and 3711 upregulated, and 396 and 1738 downregulated genes

Table 3. Summary of CNVs in ANF and MPNST

Type of Tumor (number of samples)	Median Number of CNVs per Tumor (range)	Median Size of CNV in Kb (range)	Median Number of Bases in All CNVs in Mb (range)	Percent of the Affected Part of the Genome per Tumor (range)
ANF (26)	48 (4–555)	70 (0.6–25,188)	37 (0.5–160)	0.62 (0.01- 2.66)
MPNST (28)	323 (73–4946)	275 (0.7–138,465)	1234 (152–3017)	20.6 (2.5–50.3)

in ANF and MPNST, respectively. Overlapping analysis between ANF and MPNST revealed 787 up- and 127 downregulated genes in common. Both overlaps were highly statistically significant by the hypergeometric test. There were 30 known cancer genes among the genes in these overlaps (Supplementary Table 5). *CCND1, CDK6, NRAS, MDM2*, and *MET* were among the overexpressed genes, and *AXIN2* was among the downregulated genes.

Differential Expression of Genes Frequently Affected by CNV/Mutations, Genes Identified by GSEA Leading Edge Analysis, and Select Biologically Relevant Genes

To better understand the transition of expression profiles from normal tissues to a premalignant state in ANF, we have included RNAseq data for 23 primary Schwann cell cultures established from NF1-associated PNs and enriched for *NF1*$^{-/-}$ cells. First, we compared expression of 12 genes, including *NF1, CDKN2A/B, SMARCA2, NRAS,* PRC2 genes, *CCND1, CDK6, MDM2, TP53* in PN, ANF, MPNST, and normal tissues (Figure 3). In addition, we explored differential expression of genes associated with these 12 genes through participation in protein complexes (eg, SWI/SNF, PRC1/2) or signaling pathways (eg, cell cycle, TP53) (Supplementary Figure 6). We observed highly statistically significant overexpression of *NRAS* (but not *K*- and *HRAS*) in all 3 types of tumors: PN, ANF, and MPNST. Cell-cycle inhibitors *CDKN2A* and *CDKN2B* were expressed at very low levels in normal tissues, as expected. Sharply increased expression of these 2 genes in PN is likely due to inactivation of *NF1* and subsequent activation of *RAS*, which in turn mediates oncogene-induced senescence (see Discussion). In ANF and MPNST, where frequent deletion of the *CDKN2A/B* locus was observed, expression of these genes was predictably lower than in PN, but still higher than in normal tissues. We confirmed these observations by performing IHC analysis of PN, ANF, and MPNST using anti–p16-INK4A antibodies. One can observe a robust expression of CDKN2A in most PNs and substantially lower levels of this protein in ANF and MPNST (Supplementary Figure 7). However, we observed a wide spectrum of intensities of p16 staining in the tumors, thus p16-INK4A IHC should be used in combination with other clinical and molecular analyses. Expression of cyclins D1 and D2 (*CCND1*/2) and *CDK4/6*, which control G1/S transition, was significantly higher in all 3 types of tumors compared with normal tissues (Supplementary Figure 6A). We observed elevated expression of *MDM2* in all types of tumors as well; however, expression of *TP53*, which is the target of *MDM2* suppression, was mainly unchanged in the tumors (Supplementary Figure 6B). We found that expression of *SUZ12* and *EED* was not significantly affected in the tumors; however, *EZH2*, the catalytic subunit of PRC2, was highly overexpressed in MPNST. In contrast, in ANF, expression of *EZH2* was similar to the normal controls (Supplementary Figure 6C). Expression of *SMARCA2* in ANF was essentially the same as in normal tissues (Figure 3, Supplementary Figure 6E), despite the observation that the gene was heterozygously deleted in 42%

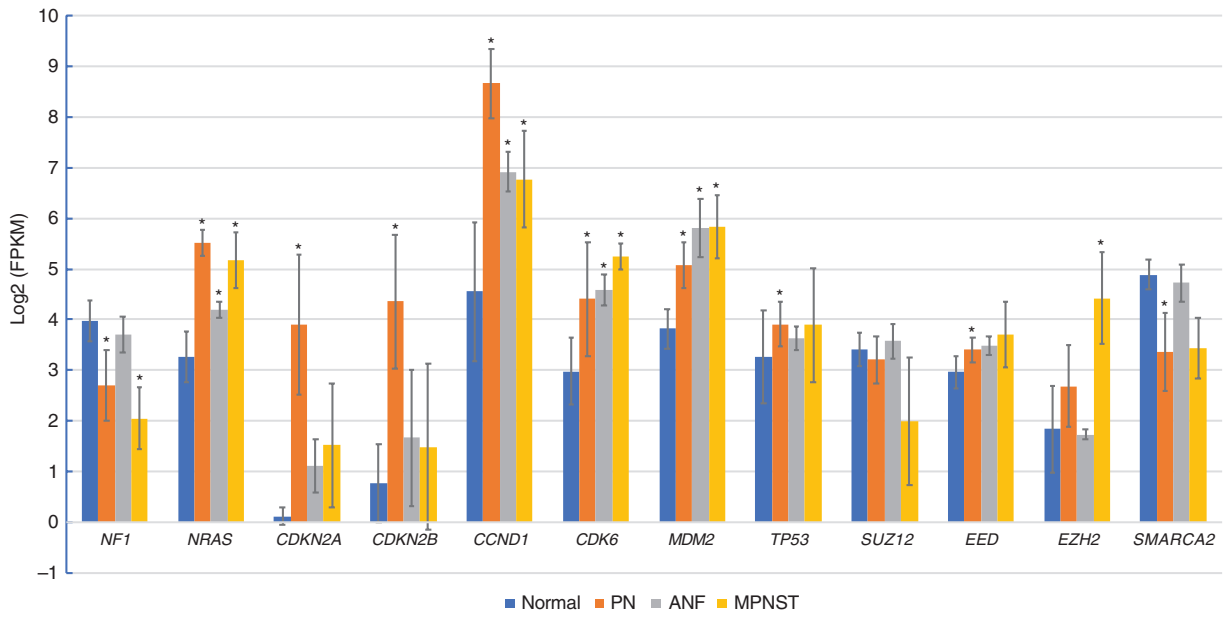

Fig. 3 Expression of genes frequently affected by CNV/mutations, genes identified by GSEA leading edge analysis, and select biologically relevant genes in normal tissues ($n = 39$), PN ($n = 23$), ANF ($n = 5$), and MPNST ($n = 5$) as determined by RNAseq analysis. Expression values are shown in fragments per kilobase per million (FPKM) reads, log2 transformed, log2(FPKM) units. Blue, red, gray, and orange bars correspond to normal tissues, PN, ANF, and MPNST, respectively. Asterisks indicate statistically significant difference (by 2-tailed *t*-tests) between normal and PN, ANF, or MPNST expression values at $P < 0.0001$.

of the tumors. However, examination of the samples, which were used for the expression analysis, has shown that only 1 of 5 samples carried heterozygous deletion of *SMARCA2*. In addition, ANFs are heterogeneous tumors with a substantial proportion of nontumor cells, which further challenges accurate estimation of gene expression in these tumors. A modest but statistically significant downregulation of *SMARCA2* in the PNs (Figure 3) warrants further investigation.

Discussion

This report is the first to describe comprehensive multiplatform genomic analyses of NF1-associated atypical neurofibromas from multiple patients. We show that *NF1* and *CDKN2A/B* loss are the primary genetic drivers in the development of ANF. In ANF, we observed *SMARCA2* loss in 42% of samples; we did not observe mutation or copy-number changes in *TP53* or the PRC2 complex. The overall somatic mutation burden in the ANFs was low and similar to that observed in PN.[15] However, unlike in PN, where chromosomal architecture is essentially normal,[15] we detected frequent (69%) deletions in chromosome 9p, which included *CDKN2A/B*. Overall, we observed a relatively low level of genomic instability in ANF and a profound, significantly increased perturbation of chromosomal architecture in MPNST, resulting in frequent gains of 178 oncogenes and in frequent losses in 144 TSGs. Gene expression analysis with RNAseq revealed upregulated *NRAS*, *MDM2*, *CCND1/2/3*, and *CDK4/6* in both ANF and MPNST, but *CCNA/E/B*, *CDK2/1*, and *EZH2* as well as the genes controlling mitosis were overexpressed in MPNST only. We provide a case report of 2 genomically distinct ANFs (both harboring 9p [*CDKN2A/B*] deletions) that arose as radiographically distinct nodular lesions from the same PN in a child with NF1.

Nielsen and colleagues[14] observed that benign neurofibromas expressed p16, whereas the MPNSTs were essentially p16 negative. They concluded that inactivation of *CDKN2A* is associated with malignant transformation of neurofibromas. The most comprehensive study of ANF to date found one highly recurrent (15/16) deletion of the *CDKN2A/B* locus.[10] A recent study has demonstrated that there is normal status of *CDKN2A/B* in PN but a deletion of this locus in 2 ANFs resected from the same patient and that, importantly, a copy-number status of *CDKN2A/B* correlated with a degree of histological atypia in these ANFs.[30] Consistent with the previous studies, we identified hetero- or homozygous deletion of the *CDKN2A/B* locus as the most frequent genetic aberration in ANF tumors and one of the most frequent in MPNST.

In addition to frequent loss of *CDKN2A/B*, we found deletion of *SMARCA2* in 42% of ANF; moreover, in at least 3 samples the *SMARCA2* deletion was clearly separate from the *CDKN2A/B* loss, pointing to a possible causative role of SWI/SNF complex disruption in the tumors. *SMARCA2* is an integral part of the ATP-dependent chromatin remodeling and transcriptional activator complex SWI/SNF, which in many instances acts as an antagonist of PRC1 and PRC2.[31] Given that the *CDKN2A/B* locus is itself a target for PRC1/2 inactivation,[32] heterozygous deletion of *SMARCA2* may lead to a partial inactivation of the SWI/SNF complex, which in turn may lower activity of p16-INK4a/b and p14-ARF by establishing a more repressive chromatin structure by PRC1/2 at this locus. It will be important to further investigate what role inactivation of *SMARCA2* and other SWI/SNF genes might play in clinical severity of ANF.

In a first, we conducted RNAseq on ANFs. We acknowledge that the number of samples in our study was modest. Consistent with clinical observations that demonstrated continuous growth of ANF,[8,9,33] we detected elevated expression of *NRAS, CCND1/2/3*, and *CDK4/6* in these tumors. We detected elevated levels of *CDKN2A/B* in ANF compared with normal tissues; however, this is consistent with findings that an activated Ras-MAPK pathway (which in PNs is caused by *NF1* inactivation) induces senescence by stimulating these cell-cycle inhibitors.[34] The frequent deletions of the *CDKN2A/B* locus that we observed in ANF may aid in overcoming p16-, p15-, and p14-mediated inhibition of the cell cycle in these tumors and, in turn, activate *MDM2*, which was also one of the genes with frequent gains in the MPNST and overexpressed in both types of tumors. Interestingly, in a recent study[35] it was demonstrated that *MDM2* directly binds to *EZH2* and modifies methylation of histones, thus promoting stemness and enabling cancer cell survival independently of p53. In light of these observations, inhibition of *MDM2* and/or *EZH2* in MPNST might be an appealing therapeutic strategy.

At present, the diagnosis of ANF is difficult and primarily is based on pathological examination of the tumors. A new term, "atypical neurofibromatous neoplasms of uncertain biologic potential (ANNUBP)," and diagnostic criteria have been recently proposed.[20] In this study, we evaluated 2 distinct ANFs (ANF14-1 and ANF14-2) from an NF1 patient and arising from the same PN. Although clinically both lesions were worrisome, the pathology examination classified only one tumor as an ANF, while deeming the other as benign neurofibroma. Subsequent genomic analysis of the tumors revealed that both lesions had concerning *CDKN2A/B* locus deletion. Careful reexamination of the tumors by the pathologist left the diagnoses unchanged; however, based on clinical and genetic evidence, we believe that both tumors should be treated as ANF. This example underscores the importance of genetic information in clinical decision making and illustrates that PN-ANF transformation could be relatively frequent, at least in some patients.

In conclusion, in our data, in addition to PN-related *NF1* inactivation, transition from benign PN to premalignant ANF frequently proceeds through inactivation of *CDKN2A/B*. *CDKN2A/B* appears to be the primary driver of this transition, but perhaps other genetic events (eg, deletion of *SMARCA2*) are also involved. Upon further transformation to the malignant state the level of genomic instability rises dramatically, accelerating complete loss of function of key gatekeepers via loss of heterozygosity (eg, *EED*, *SUZ12*) and by affecting copy number of multiple oncogenes and TSGs.

The content of this publication does not necessarily reflect the views or policies of the Department of Health and Human Services, nor does mention of trade names, commercial products, or organizations imply endorsement by the US government.

Supplementary Material

Supplementary data are available at *Neuro-Oncology* online.

Keywords

atypical neurofibromas | benign-to-malignant transformation | malignant peripheral nerve sheath tumor | neurofibromatosis type 1 | plexiform neurofibromas

Funding

This work was supported by the Intramural Research Program of the Division of Cancer Epidemiology and Genetics and the Center for Cancer Research of the National Cancer Institute, Bethesda, Maryland, the Intramural Research Program of the National Human Genome Research Institute, Bethesda, Maryland; NIH grant R29 #NS31550 (to MRW); Department of Defense DAMD 179810689 (to MRW) and Children's Tumor Foundation Neurofibroma Therapeutics Acceleration Award (to MRW).

Conflict of interest statement. The authors declare no conflicts of interest.

Authorship statement. AP—performed experiments, analyzed data, wrote and prepared manuscript for publication, submitted manuscript for publication; NFH, SS, RP, BZ—analyzed high-throughput data, wrote portion of the manuscript; CSH—collected and analyzed clinical data, wrote portion of the manuscript; ED—analyzed clinical data, wrote portion of the manuscript; MMM—performed pathology analysis of tumors; PF—prepared tumor tissues for pathology analysis; HB—collected surgical material, isolated DNA from blood and tumors, collected and analyzed clinical data; SC—performed SNP-microarray experiments, wrote portion of the manuscript; KJ—performed high-throughput experiments, wrote portion of the manuscript; JSW—wrote portion of the manuscript; JCM—contributed to experimental design and its implementation; JK—contributed to experimental design, its implementation, and interpretation of the data; EL, MRW—provided biospecimens, contributed to experimental design and interpretation of the data; BCW—provided biospecimens, contributed to experimental design and its implementation, wrote portion of the manuscript; DRS—contributed to experimental design, its implementation and interpretation of the data, wrote portion of the manuscript.

References

1. Uusitalo E, Leppävirta J, Koffert A, et al. Incidence and mortality of neurofibromatosis: a total population study in Finland. *J Invest Dermatol.* 2015;135(3):904–906.
2. Friedman JM. GeneReviews®. Pagon RA et al, eds. Seattle: University of Washington; 1993.
3. Evans DG, O'Hara C, Wilding A, et al. Mortality in neurofibromatosis 1: in North West England: an assessment of actuarial survival in a region of the UK since 1989. *Eur J Hum Genet.* 2011;19(11):1187–1191.
4. Uusitalo E, Rantanen M, Kallionpää RA, et al. Distinctive cancer associations in patients with neurofibromatosis type 1. *J Clin Oncol.* 2016;34(17):1978–1986.
5. Evans DG, Baser ME, McGaughran J, Sharif S, Howard E, Moran A. Malignant peripheral nerve sheath tumours in neurofibromatosis 1. *J Med Genet.* 2002;39(5):311–314.
6. Mautner VF, Asuagbor FA, Dombi E, et al. Assessment of benign tumor burden by whole-body MRI in patients with neurofibromatosis 1. *Neuro Oncol.* 2008;10(4):593–598.
7. Kim A, Stewart DR, Reilly KM, Viskochil D, Miettinen MM, Widemann BC. Malignant peripheral nerve sheath tumors state of the science: leveraging clinical and biological insights into effective therapies. *Sarcoma.* 2017;2017:7429697.
8. Meany H, Dombi E, Reynolds J, et al. 18-fluorodeoxyglucose-positron emission tomography (FDG-PET) evaluation of nodular lesions in patients with Neurofibromatosis type 1 and plexiform neurofibromas (PN) or malignant peripheral nerve sheath tumors (MPNST). *Pediatr Blood Cancer.* 2013;60(1):59–64.
9. Higham CS, Dombi E, Rogiers A, et al. The characteristics of 76 atypical neurofibromas as precursors to neurofibromatosis 1 associated malignant peripheral nerve sheath tumors. *Neuro Oncol.* 2018;20(6):818–825.
10. Beert E, Brems H, Daniëls B, et al. Atypical neurofibromas in neurofibromatosis type 1 are premalignant tumors. *Genes Chromosomes Cancer.* 2011;50(12):1021–1032.
11. Berner JM, Sørlie T, Mertens F, et al. Chromosome band 9p21 is frequently altered in malignant peripheral nerve sheath tumors: studies of CDKN2A and other genes of the pRB pathway. *Genes Chromosomes Cancer.* 1999;26(2):151–160.
12. Kourea HP, Orlow I, Scheithauer BW, Cordon-Cardo C, Woodruff JM. Deletions of the INK4A gene occur in malignant peripheral nerve sheath tumors but not in neurofibromas. *Am J Pathol.* 1999;155(6):1855–1860.
13. Mantripragada KK, Spurlock G, Kluwe L, et al. High-resolution DNA copy number profiling of malignant peripheral nerve sheath tumors using targeted microarray-based comparative genomic hybridization. *Clin Cancer Res.* 2008;14(4):1015–1024.
14. Nielsen GP, Stemmer-Rachamimov AO, Ino Y, Moller MB, Rosenberg AE, Louis DN. Malignant transformation of neurofibromas in neurofibromatosis 1 is associated with CDKN2A/p16 inactivation. *Am J Pathol.* 1999;155(6):1879–1884.
15. Pemov A, Li H, Patidar R, et al; NISC Comparative Sequencing Program; NCI DCEG Cancer Genomics Research Laboratory. The primacy of NF1 loss as the driver of tumorigenesis in neurofibromatosis type 1-associated plexiform neurofibromas. *Oncogene.* 2017;36(22):3168–3177.
16. Lee W, Teckie S, Wiesner T, et al. PRC2 is recurrently inactivated through EED or SUZ12 loss in malignant peripheral nerve sheath tumors. *Nat Genet.* 2014;46(11):1227–1232.
17. Zhang M, Wang Y, Jones S, et al. Somatic mutations of SUZ12 in malignant peripheral nerve sheath tumors. *Nat Genet.* 2014;46(11):1170–1172.

18. De Raedt T, Beert E, Pasmant E, et al. PRC2 loss amplifies Ras-driven transcription and confers sensitivity to BRD4-based therapies. *Nature.* 2014;514(7521):247–251.
19. Reilly KM, Kim A, Blakely J, et al. Neurofibromatosis type 1-associated MPNST state of the science: outlining a research agenda for the future. *J Natl Cancer Inst.* 2017;109(8):djx124.
20. Miettinen MM, Antonescu CR, Fletcher CDM, et al. Histopathologic evaluation of atypical neurofibromatous tumors and their transformation into malignant peripheral nerve sheath tumor in patients with neurofibromatosis 1—a consensus overview. *Hum Pathol.* 2017;67:1–10.
21. Cibulskis K, Lawrence MS, Carter SL, et al. Sensitive detection of somatic point mutations in impure and heterogeneous cancer samples. *Nat Biotechnol.* 2013;31(3):213–219.
22. Larson DE, Harris CC, Chen K, et al. SomaticSniper: identification of somatic point mutations in whole genome sequencing data. *Bioinformatics.* 2012;28(3):311–317.
23. Hansen NF, Gartner JJ, Mei L, Samuels Y, Mullikin JC. Shimmer: detection of genetic alterations in tumors using next-generation sequence data. *Bioinformatics.* 2013;29(12):1498–1503.
24. Saunders CT, Wong WS, Swamy S, Becq J, Murray LJ, Cheetham RK. Strelka: accurate somatic small-variant calling from sequenced tumor-normal sample pairs. *Bioinformatics.* 2012;28(14):1811–1817.
25. Fuentes Fajardo KV, Adams D, Mason CE, et al; NISC Comparative Sequencing Program. Detecting false-positive signals in exome sequencing. *Hum Mutat.* 2012;33(4):609–613.
26. Van Loo P, Nilsen G, Nordgard SH, et al. Analyzing cancer samples with SNP arrays. *Methods Mol Biol.* 2012;802:57–72.
27. Sathirapongsasuti JF, Lee H, Horst BA, et al. Exome sequencing-based copy-number variation and loss of heterozygosity detection: ExomeCNV. *Bioinformatics.* 2011;27(19):2648–2654.
28. Dewan R, Pemov A, Kim HJ, et al. Evidence of polyclonality in neurofibromatosis type 2-associated multilobulated vestibular schwannomas. *Neuro Oncol.* 2015;17(4):566–573.
29. Kim M, Morales LD, Jang IS, Cho YY, Kim DJ. Protein tyrosine phosphatases as potential regulators of STAT3 signaling. *Int J Mol Sci* 2018;19.
30. Carrió M, Gel B, Terribas E, et al. Analysis of intratumor heterogeneity in Neurofibromatosis type 1 plexiform neurofibromas and neurofibromas with atypical features: correlating histological and genomic findings. *Hum Mutat.* 2018;39(8):1112–1125.
31. Kadoch C, Copeland RA, Keilhack H. PRC2 and SWI/SNF chromatin remodeling complexes in health and disease. *Biochemistry.* 2016;55(11):1600–1614.
32. Gil J, Peters G. Regulation of the INK4b-ARF-INK4a tumour suppressor locus: all for one or one for all. *Nat Rev Mol Cell Biol.* 2006;7(9):667–677.
33. Ferner RE, Golding JF, Smith M, et al. [18F]2-fluoro-2-deoxy-D-glucose positron emission tomography (FDG PET) as a diagnostic tool for neurofibromatosis 1 (NF1) associated malignant peripheral nerve sheath tumours (MPNSTs): a long-term clinical study. *Ann Oncol.* 2008;19(2):390–394.
34. DeNicola GM, Tuveson DA. RAS in cellular transformation and senescence. *Eur J Cancer.* 2009;45(Suppl 1):211–216.
35. Wienken M, Dickmanns A, Nemajerova A, et al. MDM2 associates with polycomb repressor complex 2 and enhances stemness-promoting chromatin modifications independent of p53. *Mol Cell.* 2016;61(1):68–83.